Monolithic Integration of an ARROW-Type Demultiplexer and Photodetector in the Shorter Wavelength Region

TOSHIHIKO BABA, YASUO KOKUBUN, MEMBER, IEEE, AND HIDEHIRO WATANABE

Abstract—**We have proposed and designed a monolithic integration of a novel antiresonant reflecting optical waveguide (ARROW) type demultiplexer and photodetector. The isolation was theoretically calculated to be −21.6 dB between the wavelengths of 0.78 and 0.88 μm with a maximum detecting efficiency of 58 percent in a short demultiplexing/photodetecting length of 100 μm. We demonstrated its fundamental characteristic experimentally. This type of device can be applied to a wavelength division multiplexing (WDM) system with comparatively wide wavelength separation, e.g., 1.3- and 1.55-μm wavelengths.**

I. Introduction

ONE of the key components of the wavelength division multiplexing (WDM) transmission system is a multi/demultiplexer, and many kinds of devices including prisms, thin-film filters, and diffractional gratings have been studied [1], [2]. Recently, several monolithic integrated structures using optical waveguides and directional couplers or gratings drawn by electron beam lithography were reported for the purpose of miniaturization, mass production, and stabilization of characteristics [3]–[5]. It is difficult, however, to integrate photodetectors monolithically because a sophisticated technique is necessary in order to fabricate a tapered cladding or a grating, and these are required when coupling the light from the waveguide to the photodetector that is formed in the substrate. In addition to this, the device size is as large as one centimeter because of the separate structure of the demultiplexing and photodetecting regions.

The antiresonant reflecting optical waveguide (ARROW) [6]–[8] is a novel single-mode optical waveguide on a semiconductor substrate. An interference cladding is inserted between the core and the substrate, as shown in Fig. 1, and it consists of two different films having a large index difference. We call the high-index layer the first cladding layer and the low-index layer the second cladding layer. This waveguide can maintain a single-mode propagation by the loss discrimination of higher order modes. The propagation loss of the fundamental mode has wavelength dependence resulting from the change of the resonant condition inside the interference cladding. We have applied this characteristic to a waveguide-type demultiplexer.

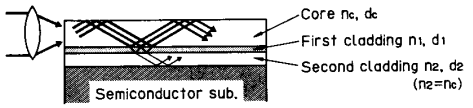

Fig. 1. Structure of ARROW.

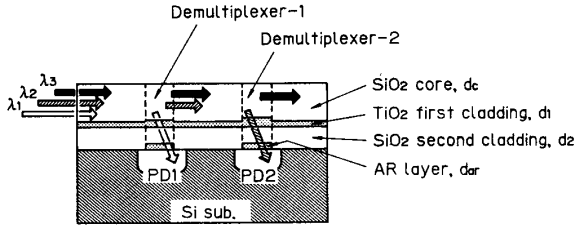

Fig. 2. Fundamental structure of ARROW-type demultiplexer and photodetector integrated device.

In this paper, we propose and investigate the potential of the monolithic integration of an ARROW-type demultiplexer and photodetector, as shown in Fig. 2. First, we design the integrated device for short wavelengths of 0.78 and 0.88 μm. We introduce an antireflecting (AR) layer in order to enhance the coupling efficiency to the photodetector. We discuss the optimum length of the photodetector and the performance of the device with the AR layer. Next, we describe the fabrication of a simplified integrated device and the measured results of the demultiplexing and photodetecting characteristics.

II. Structure

Let us define the thickness and the refractive index of each layer as they are shown in Fig. 1.

We adopted a transparent TiO_2 ($n_1 = 2.0$) for the first cladding layer and p-type silicon ($n_s = 3.6$–3.8) for the substrate. In the structure shown in Fig. 2, the multiplexed light propagates through the SiO_2 ($n_c = 1.45$–

Manuscript received November 28, 1988; revised June 7, 1989. This work was supported by the Ministry of Education, Science and Culture under Grants 63460139 and 63790296, the Hōso Bunka Foundation, KDD Engineering and Consulting Foundation, the Murata Science Foundation, the Okawa Institute of Information and Telecommunication, the Casio Science Promotion Foundation, and the Nippon Sheet Glass Foundation for Material Science.

The authors are with Yokohama National University, Faculty of Engineering, Division of Electrical and Computer Engineering, Yokohama, Japan 240.

IEEE Log Number 8931034.

1.46) core of the ARROW on low-loss condition and reaches to the demultiplexing region. In this region, the thickness of the first cladding layer is adjusted to the resonant condition on which a certain wavelength is radiated out to the photodetector fabricated in the silicon substrate. On the other hand, light having other wavelengths passes through the region with low loss. Thus this device acts as a demultiplexer/photodetector integrated device.

The light coupling from the ARROW to the photodetector is equivalent to the large radiation loss of the guided wave in the core of the ARROW. We calculated the loss characteristics by using the mode analysis method [8], which utilizes the interference matrix. Fig. 3 shows the loss characteristic of the TE fundamental mode of a typical ARROW against the thickness of the first cladding layer d_1. Here, we assumed that the thicknesses of the SiO_2 core and the second cladding layer are 4 and 2 μm, respectively. At both wavelengths (0.78 and 0.88 μm), the loss varies periodically from low loss to extremely high value as the thickness of the first cladding layer changes. The ARROW acts as a low-loss waveguide when the thickness of the first cladding layer satisfies the following antiresonant condition [6]-[8]:

$$d_1 \simeq \frac{\lambda}{4n_1}\left[1 - \left(\frac{n_c}{n_1}\right)^2 + \left(\frac{\lambda}{2n_1 d_c}\right)^2\right]^{-1/2} \cdot (2M + 1)$$
$$(M = 0, 1, 2, \cdots) \quad (1)$$

where λ is the wavelength. It is seen from Fig. 3 that the low-loss range of the ARROW is fairly broad and that d_1 of 0.16 μm is the first low-loss condition satisfied in both wavelengths simultaneously.

On the other hand, the resonant condition of d_1 on which the loss takes its maximum value is approximately expressed by [9]

$$d_1 \simeq \frac{\lambda}{2n_1}\left[1 - \left(\frac{n_c}{n_1}\right)^2\right]^{-1/2} \cdot \left[N + \frac{3\lambda}{2\pi^2 d_c \sqrt{n_1^2 - n_c^2}}\right]$$
$$(N = 0, 1, 2, \cdots). \quad (2)$$

In Fig. 3, these conditions for $\lambda = 0.78$ and 0.88 μm correspond to $d_1 = 0.30$ and 0.36 μm, respectively, for the order of resonance $N = 1$. Fig. 4 shows the wavelength dependence of propagation loss for three different thicknesses of first cladding layer d_1. The loss peaks appear at $\lambda = 0.78$ and 0.88 μm, when $d_1 = 0.30$ and 0.36 μm, respectively, according to the characteristic shown in Fig. 3. It can be seen from Fig. 4 that the slope of the loss curve in the wavelength shorter than the demultiplexing wavelength is steeper than that in the longer wavelength. This implies that we can expect high isolation by demultiplexing the longer wavelength first. When d_1 is 0.16 μm, no peculiar wavelength appears, and the loss is lower than 1 dB/cm in the broad wavelength range.

In addition, we introduced an (AR) layer on the surface of the photodetector, as is shown in Fig. 2, in order to enhance the coupling efficiency to the photodetector. The optimum index and thickness of the AR layer (n_{AR} and

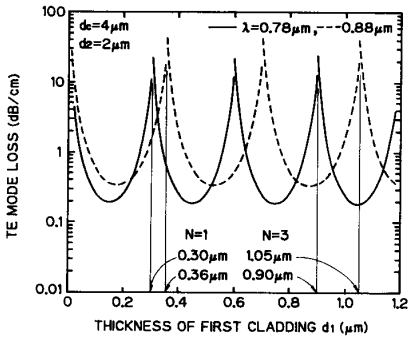

Fig. 3. Propagation loss characteristic of TE_0 fundamental mode against thickness of first cladding layer for $\lambda = 0.78$ and 0.88 μm.

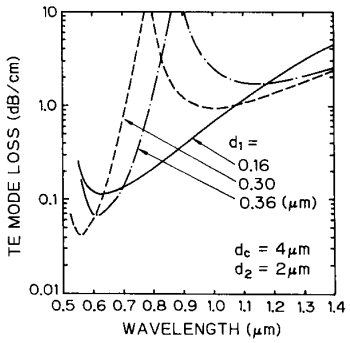

Fig. 4. Wavelength dependence of propagation loss of TE_0 fundamental.

d_{AR}) are approximately given in terms of the propagation angle of guided light in the ARROW θ by

$$n_{AR} \simeq \left[n_c^2 \cos^2\theta + n_c \sin\theta\left(n_s^2 - n_c^2\cos^2\theta\right)^{1/2}\right]^{1/2} \quad (3)$$

$$d_{AR} \simeq \frac{\lambda}{4n_{AR}}\left[1 - \left(\frac{n_c}{n_{AR}}\right)^2 \cos^2\theta\right]^{-1/2} \cdot (2L + 1)$$
$$(L = 0, 1, 2, \cdots). \quad (4)$$

Assuming a large optical confinement of the ARROW, the propagation angle of the TE fundamental mode of the ARROW θ_0 is approximately given by

$$\tan\theta_0 \simeq \left[\left(\frac{2n_c d_c}{\lambda}\right)^2 - 1\right]^{-1/2}. \quad (5)$$

In the shorter wavelength region ranging from 0.78 to 0.88 μm, θ_0 is about 3.8–4.3° when the thickness of the core is 4 μm, and optimum n_{AR} is calculated to be 1.55–1.59. In this paper, we adopted NA45 glass[1] ($n = 1.54$) for the material of this layer. Fig. 5 shows the calculated power reflectivity at the interface between the second cladding layer and the substrate when the NA45 glass AR layer is inserted. The reflection almost vanishes for both $\lambda = 0.78$ and 0.88 μm at $d_{AR} = 0.41$ μm. Owing to both the short detector length resulting from the effect of the AR layers and the demultiplexer/detector integrated configuration,

[1]Made by HOYA Corp. Composition is almost the same as C7059 glass.

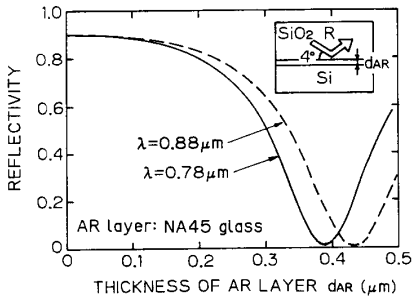

Fig. 5. Reflectivity of interface between second cladding layer and substrate to which the AR layer is inserted.

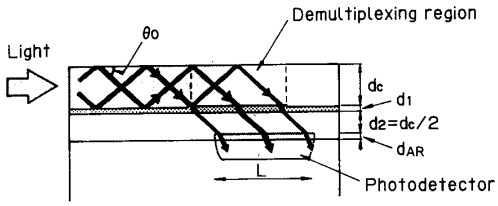

Fig. 6. Simplified model of light power transition in demultiplexing region.

the size of the integrated device can be very small (typically 100–200 μm per each demultiplexing/photodetecting region) compared with the conventional directional coupler-type and grating-type demultiplexers.

In the demultiplexing region with the AR layer having the optimum index and thickness, reflection at all interfaces under the core vanishes for the demultiplexing wavelength. Thus we can treat the radiation of light power from the core to the substrate by a simple ray model, as shown in Fig. 6. Because of the large core size of the ARROW compared with the wavelength, the first term in the parenthesis in (5) is much larger than unity. From the model shown in Fig. 6, the normalized detector length L_d/λ required to obtain a high coupling efficiency is given approximately by

$$\frac{L_d}{\lambda} \simeq 4n_c\left(\frac{d_c}{\lambda}\right)^2. \tag{6}$$

Equation (6) implies that L_d is mainly determined by the thickness of core d_c and the wavelength λ. Even when the core is as thick as 4 μm, it requires a very short detector length of about 150 μm to achieve an efficient coupling in this wavelength region. If we form the conventional structure, i.e., a light coupling from a conventional waveguide to a photodetector through a tapered cladding, more than six times the length of the detector (>1 mm) is required to achieve a high coupling efficiency for the same thickness of core.

III. Wavelength Selectivity

When assuming NA45 glass for the AR layer with the optimum thickness of 0.41 μm, the coupling efficiency from the ARROW to the photodetector against the wavelength is shown in Fig. 7. This was obtained by the wave analysis, in which the light power transition in the demultiplexing region was calculated by expanding the incident light into a continuous spectrum of radiation modes [9]–[11]. Here, we define the isolation I between the objective wavelength λ_1 and the obstructive wavelength λ_2 in a single demultiplexing region as follows:

$$I \equiv 10\log_{10}\left[\eta(\lambda_1)/\eta(\lambda_2)\right] \text{ (dB)} \tag{7}$$

where $\eta(\lambda_i)$ $(i = 1, 2)$ is the coupling efficiency from the waveguide to the photodetector. The physical meaning of this definition is that isolation of a demultiplexer is measured as a ratio of output powers of two wavelengths when the input powers of these wavelengths are the same.

Fig. 7(a) shows the coupling efficiency against the wavelength when the first cladding layer satisfies the first-

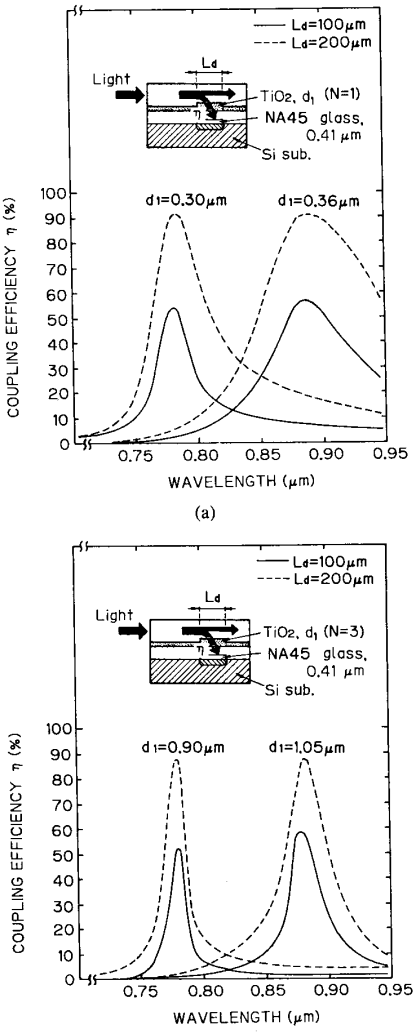

Fig. 7. Coupling efficiency from ARROW to photodetector covered with the AR layer: (a) First-order interference ($N = 1$); (b) third-order interference ($N = 3$).

order resonance condition $N = 1$, as shown in Fig. 3. The isolation I between two wavelengths (0.78 and 0.88 μm) takes a larger value for $d_1 = 0.36$ μm than for $d_1 = 0.30$ μm. This coincides with the discussion in the paragraph following (2). When $L_d = 100$ μm and $d_1 = 0.36$ μm, the value of I is evaluated to -17 dB, and the coupling efficiency reaches to about 58 percent.

This isolation can be improved by adopting higher order resonance of the first cladding layer. In Fig. 3, the thickness d_1 of 1.05 μm ($N = 3$) satisfies the demultiplexing condition for $\lambda = 0.88$ μm and the minimum loss condition for $\lambda = 0.78$ μm simultaneously. Therefore, the sharpness of the demultiplexing characteristic is improved, as is seen in Fig. 7(b). The isolation increases to -21.6 dB under the same condition as in Fig. 7(a). In general, the optimum order of resonance N is given as an integer number closest to

$$N \approx \frac{\lambda_i}{2\Delta\lambda} \qquad (i = 1 \text{ or } 2) \tag{8}$$

where $\Delta\lambda$ is the difference between λ_1 and λ_2. If all the optimum conditions for the order of resonance N and the detector length L_d given (6) are achieved, the isolation I between two wavelengths can be evaluated by

$$I \simeq 10 \log_{10} \left[1 - 10^{-\{0.217/(n_1^2 - n_c^2)\}(\lambda_2/d_c)^2\}(\lambda_2/\lambda_1)}\right] \text{ (dB)}. \tag{9}$$

Here, we assumed the absolute transparent condition of the AR layer for both λ_1 and λ_2 because the antireflecting condition is not as sensitive to the wavelength, as is seen in Fig. 5. It is seen from (9) that a larger index difference between the first cladding and core and the larger core size can achieve larger isolation. Therefore, semiconductor materials such as Si, which have a very high index ($n = 3.5$) and small absorption, are more suitable for the first cladding layer in the 1.3–1.6 μm wavelength region. For example, the isolation is calculated from (9) to -29.6 dB between the obstructive wavelength of 1.3 μm and the objective wavelength of 1.55 μm for $N = 3$, assuming Si as the first cladding and $d_c = 8$ μm, which is the typical core size of single-mode optical fibers.

IV. Fabrication and Measurement

In order to measure the fundamental demultiplexing characteristic of the integrated device clearly, we fabricated a simplified structure, as illustrated in Fig. 8, which includes several separate devices in one substrate. Each device has a single demultiplexing and photodetecting region with a straight-channel waveguide. If we measure the characteristics of the tandem device as shown in Fig. 2, the measured characteristics of the rear device will be affected by the front device. Thus we cannot precisely measure the isolation defined by (7).

The fabrication process is as follows. First, phosphorus was diffused into the p-type silicon substrate through a thermally oxidized mask (0.8-μm thick) to turn a p-n junction into photodetectors. In this diffusion process, we spincoated a solvent containing phosphorus[2] and heated it to 1000° C for 1 h in a nitrogen atmosphere. Next, an NA45 glass AR layer ($d_{AR} = 0.41$ μm) was sputtered in a gas mixture of argon and oxygen and was removed (except for the surface of the photodetector) by a chemical etching. Then, an SiO_2 second cladding ($d_2 = 2$ μm) was sputtered under the same conditions as was the NA45 glass. Aluminum was evaporated onto this layer, and electrode patterns were formed to be n-side electrodes contacting with photodetectors through contact hales. A TiO_2 first cladding layer was formed by an electron-beam evaporation in a 1×10^{-4}-torr oxygen atmosphere. The thickness of this layer was changed by using a lift-off technique for two regions: one for the waveguide region and the other for the demultiplexer region. The thickness at the waveguide region was 0.16 μm. In the demultiplexing region, we designed two thicknesses: $d_1 = 0.30$ μm for $\lambda = 0.78$ μm and $d_1 = 0.36$ μm for $\lambda = 0.88$ μm, respectively. The length of the demultiplexing region was 100 μm. Last, a 4-μm thick SiO_2 core was sputtered, and ridge waveguides 20-μm wide and 1.5 μm of step height were formed by chemical etching. The waveguide length was 1.0 cm. A cross-sectional view of the waveguide and a top view of fabricated device are shown in Fig. 9.

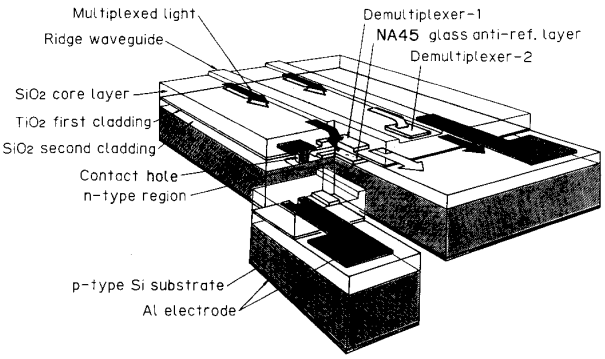

Fig. 8. Fabricated structure of integrated device.

The experimental setup for measurement is shown in Fig. 10. The demultiplexing characteristic was measured by using several semiconductor lasers with different wavelengths ranging from 0.78 to 0.89 μm. The laser beam ($P = 2$ mW) with TE polarization was focused onto the cleaved-end facet of the device. (We also tried to measure the characteristic for TM polarization. However, the incident light could hardly be guided through the waveguide due to large polarization dependence of the propagation loss of the ARROW [6], [8].) The demultiplexed light radiated out to the substrate was detected by the p-n junction on which the inverse bias voltage of 5 V was applied. The observed light intensity was converted to the total quantum efficiency, which is defined as the ratio of the number of produced carriers and the number of incident photons.

[2]OCD-P, which is made by Tokyo Ohka Kogyo Co., Ltd.

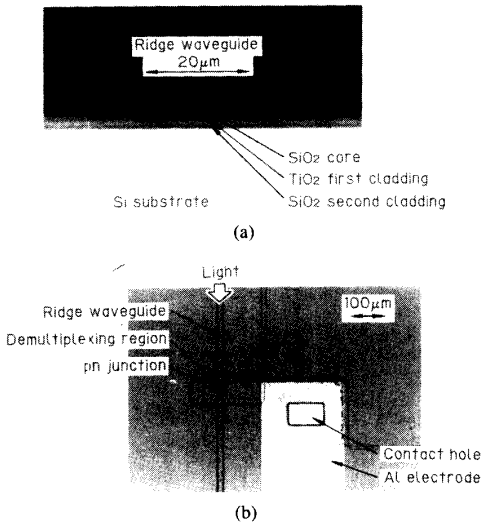

Fig. 9. Photographs of fabricated device: (a) Cross-sectional view of waveguide; (b) top view.

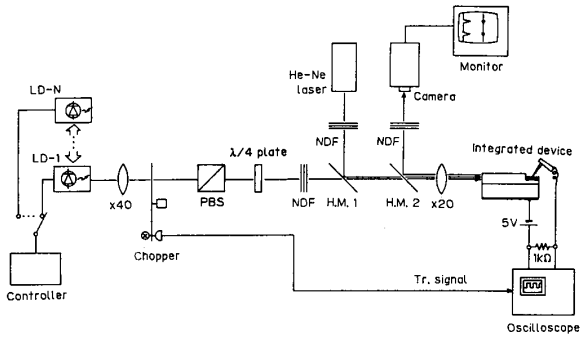

Fig. 10. Experimental setup for measurement.

Fig. 11 shows the measured results of two devices, i.e., for the wavelengths of 0.78 and 0.88 μm, which were fabricated simultaneously on the same substrate. In Fig. 11(a), the peak point of the output signal appeared clearly at $\lambda = 0.82$ μm for the 0.78-μm demultiplexer. In contrast to this, the output signal from the 0.88-μm demultiplexer increased monotonously against the wavelength, and the peak wavelength seems to have shifted to longer than 0.9 μm, as is shown in Fig. 11(b). The sensitivity of the photodetector was measured independently by illuminating the photodetector surface directly. The measured quantum efficiency decreased gradually against the wavelength, as is shown in Fig. 12. The decline of the efficiency at $\lambda = 0.86$ μm seems to have been caused by the interference of multilayer films on the surface. These results imply that the first cladding layers in both samples were thicker than the designed values. From the peak wavelength, the thickness of the 0.78-μm demultiplexer was evaluated to be 0.32 μm (7-percent thicker than the designed value). Anyway, it was confirmed from these characteristics that this device has a fundamental demultiplexing function. The isolation is evaluated to be -5.4 dB when the wavelength separation is 40 nm.

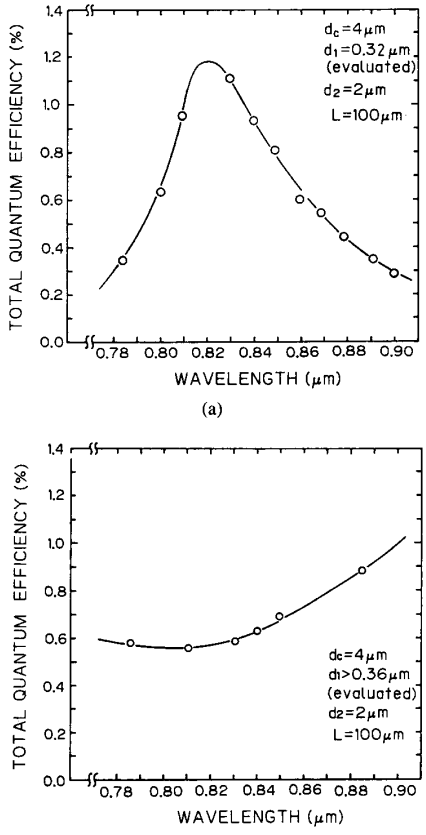

Fig. 11. Measured demultiplexing characteristics against wavelength: (a) Designed for $\lambda = 0.78$ μm; (b) designed for $\lambda = 0.88$ μm.

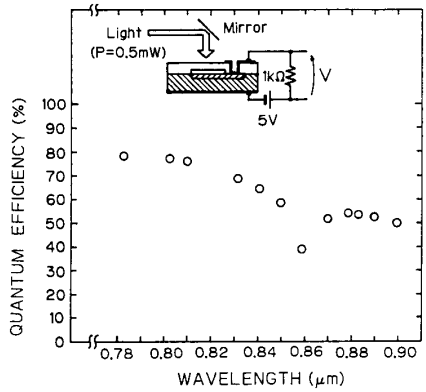

Fig. 12. Measured quantum efficiency of fabricated photodetector against wavelength.

The maximum total quantum efficiency was about 1.1 percent. This small value seems to be attributed to large coupling loss at the input end and large propagation loss through the waveguide. The former was due to the mismatch of field profiles between the waveguide (cross section was 4×20 μm), and the focused circular spot and was calculated to be 4.5 dB. The latter was caused by

scattering resulting from many pinholes on the surface of the core and some irregularities of the ridge waveguide pattern. From the attenuation of scattered light along the propagation axis, the waveguide loss was evaluated from 7 to 10 dB. The reduction of these losses will be possible by introducing a novel three-dimensional ARROW using stripe lateral confinement [12]. Low-loss single-mode propagation, circular-spot profile, and easy fabrication will be achieved by this waveguide structure. Taking into account these losses and the quantum efficiency of the photodetector shown in Fig. 12, the coupling efficiency of the selected wavelength to the photodetector is evaluated to be about 20–40 percent.

Besides these losses, the output level that is far from the peak wavelength is higher than the theoretical value, particularly in the wavelength region that is longer than the peak wavelength. This seems to be caused by light scattering from a step of the core surface, which exists at the boundary between the waveguide region and the demultiplexing region. The improvement of the total quantum efficiency and the isolation seems to be possible by smoothing the surface roughness of the fabricated waveguide and by burying the AR layer into the substrate.

V. Summary

The monolithic integration of a novel ARROW-type demultiplexer and photodetector has been proposed and demonstrated. The isolation between the wavelengths of 0.78 and 0.88 μm was calculated to be -21.6 dB at the optimum resonance condition. The fundamental demultiplexing function was observed in the 0.78–0.89-μm wavelength range, and the isolation was evaluated to be -5.4 dB when the wavelength separation was 40 nm. This type of device can be applied to a WDM system with comparatively wide wavelength separation, e.g., 1.3- and 1.55-μm wavelengths.

Acknowledgment

The authors would like to express their sincere thanks to Prof. K. Iga, T. Sakaguchi, and H. Uenohara of the Tokyo Institute of Technology for the use of the electron beam evaporator and the optical spectrum analyzer. They would also like to thank Prof. M. Toki and Prof. Y. Tsuzuki of Yokohama National University for their support. They also thank Dr. N. Haneji of Yokohama National University, Dr. H. Nakajima and Dr. M. Seino of Fujitsu Laboratories, and K. Yokomori and T. Kihara of Ricoh Corp. for their help with the experiment.

References

[1] G. Winzer, "Wavelength multiplexing components—A review of single-mode devices and their applications," *J. Lightwave Technol.*, vol. LT-2, p. 369, 1984.

[2] H. Ishio, J. Minowa, and K. Nosu, "Review and status of wavelength-division multiplexing technology and its application," *J. Lightwave Tech.*, vol. LT-2, p. 448, 1984.

[3] T. Suhara, J. Viljanen, and M. Leppihalme, "Integrated-optic wavelength multi and demultiplexers using a chirped grating and an ion exchanged waveguide," *Appl. Opt.*, vol. 21, p. 2195, 1982.

[4] N. Takato, Y. Otsuka, K. Jinguji, M. Yasu, and M. Kawachi, "Guided-wave multi/demultiplexers for 1.3/1.5 μm wavelengths using directional couplers by high-silica waveguides," in *Nat. Conf. Rec. 1986 Opt. Radio Wave Electron.*, IECEJ, no. 255, 1986.

[5] K. Imoto, H. Uetsuka, and H. Sano, "Guided-wave multi/demultiplexers with high stopband rejection," *Appl. Opt.*, vol. 26, p. 4214, 1987.

[6] M. A. Duguay, Y. Kokubun, T. L. Koch, and L. Pfeiffer, "Antiresonant reflecting optical waveguides in SiO_2-Si multilayer structures," *Appl. Phys. Lett.*, vol. 49, p. 13, 1986.

[7] Y. Kokubun, T. Baba, T. Sakaki, and K. Iga, "Low loss antiresonant reflecting optical waveguide on Si substrate in visible wavelength region," *Electron. Lett.*, vol. 22, p. 892, 1986.

[8] T. Baba, Y. Kokubun, T. Sakaki, and K. Iga, "Loss reduction of an ARROW waveguide in shorter wavelength and its stack configuration," *J. Lightwave Tech.*, vol. 6, p. 1440, 1988.

[9] T. Baba and Y. Kokubun, "High efficiency coupling from ARROW to photodetector integrated into substrate," *Appl. Opt.*, to be published.

[10] Y. Suematsu and K. Furuya, "Quasi-guided modes and radiation losses in optical dielectric waveguides with external higher index surroundings," *IEEE Trans. Microwave Theory Tech.*, vol. MTT-23, p. 170, 1975.

[11] A. K. Ghatak, K. Thyagarajan, and M. R. Shenoy, "Numerical analysis of planar optical waveguides using matrix approach," *J. Lightwave Technol.*, vol. LT-5, p. 660, 1987.

[12] T. Baba, Y. Kokubun, and Y. Mera, "A novel 3-dimensional ARROW by thin film patterning—Stripe lateral confinement of ARROW—," *Tenth Topical Mtg. Integrated Guided Wave Optics* (Houston), no. TuBB-5, 1989.

[13] T. L. Koch, P. J. Corvini, W. T. Tsang, U. Koren, and B. I. Miller, "Wavelength selective interlayer directionally grating-coupled InP/InGaAsP waveguide photodetection," *Appl. Phys. Lett.*, vol. 51, p. 1060, 1987.

*

Toshihiko Baba was born in Ueda City in Nagano Prefecture, Japan, on November 12, 1962. He received the B.E. degree in electrical engineering and the M.E. degree in electrical and computer engineering from the Yokohama National University, Yokohama, Japan, in 1985 and 1987, respectively.

He is currently working towards the Dr.Eng. degree at the Graduate School of Yokohama National University.

Mr. Baba is a member of the Institute of Electronics, Information and Communication Engineers and the Japan Society of Applied Physics.

*

Yasuo Kokubun (M'85) was born in Fukushima Prefecture, Japan, on July 7, 1952. He received the B.E. degree from Yokohama National University, Yokohama, Japan, in 1975 and the M.E. and Ph.D. degrees from Tokyo Institute of Technology, Tokyo, Japan, in 1977 and 1980, respectively.

After he worked for the Research Laboratory of Precision Machinery and Electronics, Tokyo Institute of Technology, as an Research Associate from 1980 to 1983, he joined the Yokohama National University as an Associate Professor in 1983. His current research is in integrated optics, especially waveguide-type optical devices. From 1984 to 1985, he was with AT&T Bell Laboratories, Holmdel, NJ, as a Member of Technical Staff and was engaged in a novel waveguide on semiconductor substrate (ARROW) for integrated optics.

Dr. Kokubun is a member of the Institute of Electronics, Information, and Communication Engineers, the Japan Society of Applied Physics, and the Optical Society of America.

*

Hidehiro Watanabe was born in Shizuoka Prefecture, Japan, on July 3, 1966. He received the B.E. degree in electrical and computer engineering from Yokohama National University, Yokohama, Japan, in 1988.

He is now working towards the M.E. degree at the Graduate School of Yokohama National University.

Mr. Watanabe is a member of the Institute of Electronics, Information, and Communication Engineers.